Electronic Supplementary Information (ESI)

Ion-controlled three-color fluorescent telomeric switch on DNA origami

L. Olejko[a, b, c], P. J.Cywiński[d, e] and I. Bald[a, c]

[a.] Department of Chemistry, Physical Chemistry, University of Potsdam, Karl-Liebknecht Str. 24-25, 14476 Potsdam, Germany

[b.] School of Analytical Sciences Adlershof, Humboldt-Universität zu Berlin, Unter den Linden 6, 10099, Germany

[c.] BAM Federal Institute for Materials Research and Testing, Richard-Willstätter Str. 11, 12489 Berlin, Germany

[d.] Fraunhofer IAP, Geiselbergstrasse 69, 14476 Potsdam, Germany

[e.] Institute of Physical Chemistry, Polish Academy of Sciences, Kasprzaka 44/53, 01-224 Warsaw, Poland

HumTel and RevHumTel on DNA origami structures

FAM fluorescence decays for HumTel and RevHumTel on DNA origami structures are shown in Fig. S1. The fluorescence decay time for HumTel (blue decay, τ = 3.2 ns) decreases after KCl (black decay, τ = 1.5 ns) and NaCl (brown decay, τ = 1.6 ns) addition (Fig. S1 A). The G-quadruplex folds in presence of both salts. For RevHumTel on the other hand the fluorescence decay time is only influenced by KCl (without salt: blue decay, τ = 3.1 ns; KCl: black decay, τ = 1.8 ns; NaCl: brown decay, τ = 2.9 ns, (Fig. S1 B)). RevHumTel attached to DNA origami structures is selective for K^+. The G-quadruplex cannot fold in presence of Na^+ on DNA origami structures.

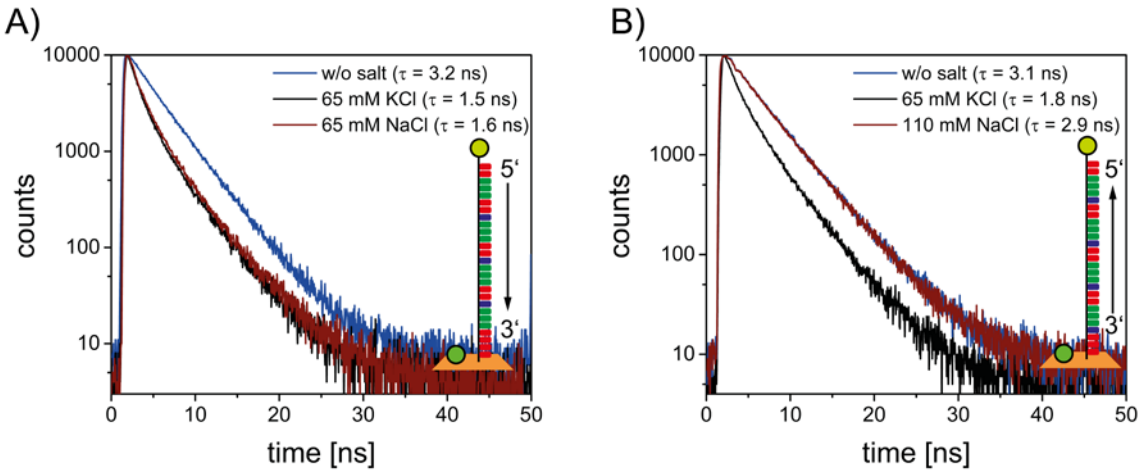

Fig. S 1 *FAM fluorescence decays (λ_{ex} = 490 nm, λ_{em} = 520 nm) for DNA origami triangles modified with two different telomeric DNA sequences: HumTel (A) and RevHumTel (B) before (blue) and after KCl (black) and NaCl (brown) addition. RevHumTel folds into G-quadruplex structures only in presence of KCl (NaCl does not influence FAM fluorescence decay time).*

Ion-selectivity of RevHumTel on DNA origami structures

The reversed human telomere shows a high selectivity only for KCl. Other monovalent cations such as Na^+, Li^+, Cs^+ and NH_4^+ do not influence the FRET efficiency and therefore do not induce G-quadruplex formation (Fig. S2). Divalent cations such as Mg^{2+} and Ca^{2+} influence the FRET efficiency (Fig. S2) and stabilize G-quadruplex structures.[1,2] Since the $MgCl_2$ concentration for the DNA origami preparation is as low as 10 mM in the present case and does not increase throughout the experiments, only a small constant number of Mg^{2+}-induced G-quadruplexes is present.

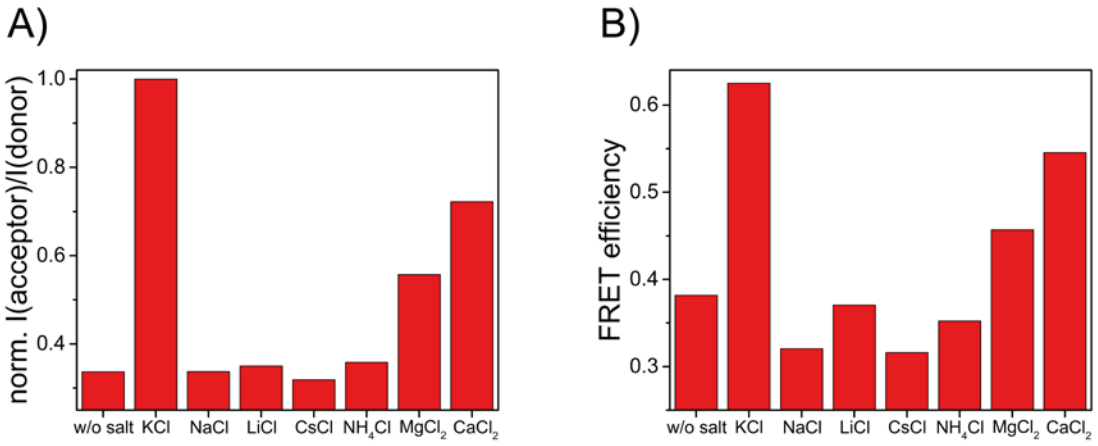

Fig. S 2 *RevHumTel shows a high selectivity towards potassium. The FRET process is only turned on after KCl addition. Other monovalent cations (Na^+, Li^+, Cs^+ and NH_4^+) do not induce a G-quadruplex formation. Only divalent cations such as Mg^{2+} and Ca^{2+} have an influence on the FRET process. A) Results for steady state fluorescence measurements (λ_{ex} = 450 nm). Normalized donor-acceptor-ratios (I(565 nm/I(515 nm) after the addition of 110 mM salt (except $MgCl_2$: 120 mM). B) FRET efficiencies calculated with FAM decay times after salt addition (c = 110 mM, except $MgCl_2$: c = 120 mM).*

G-quadruplex unfolding using 18-crown-6

In this study, we use cryptand to remove K^+ and unfold the G-quadruplex. Other complexing agents can also be used such as 18-crown-6. This crown ether can also encapsulate K^+ and therefore unfold the G-quadruplex. Steady state and time-resolved fluorescence data for one switching cycle using 18-crown-6 in the two-color FRET system are shown in Fig. S3. To unfold the G-quadruplex and turn off the energy transfer from FAM to Cy3 comparatively high amounts of 18-crown-6 are needed (for 22 mM KCl 130 mM 18-crown-6). Therefore, cryptand is used in this study to unfold the G-quadruplex.

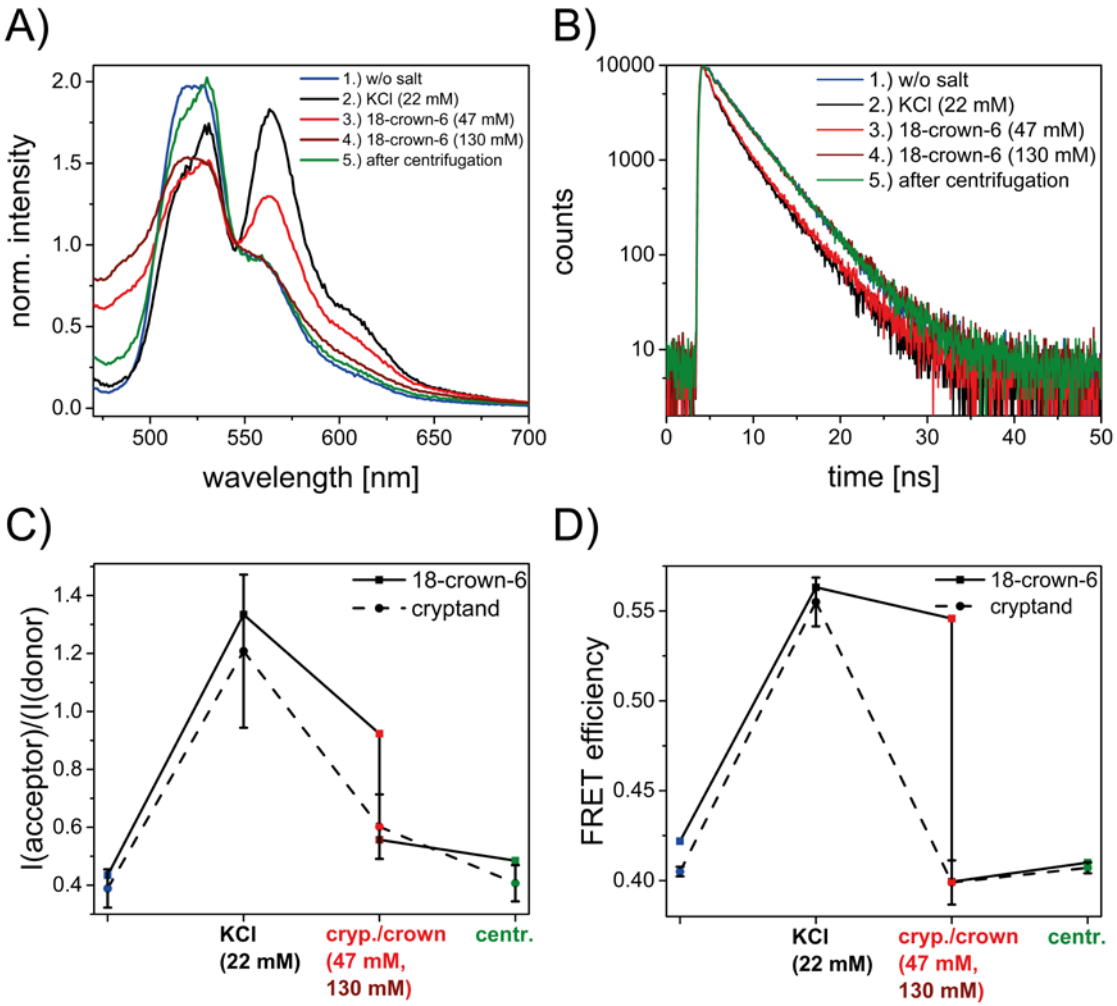

Fig. S 3 *FRET switching of two-color FRET system using 18-crown-6. A) Normalized emission spectra (λ_{ex} = 450 nm) before (blue), after KCl (black) and after 18-crown-6 (47 mM: red; 130 mM: brown) addition and after centrifugation (green). The G-quadruplex unfolds after 18-crown-6 addition and the FRET process is turned off. A high concentration of 18-crown-6 is needed to unfold the G-quadruplex. B) Fluorescence decays (λ_{ex} = 490 nm, λ_{em} = 520 nm) before (blue), after KCl (black) and after 18-crown-6 (47 mM: red, 130 mM: brown) addition and after centrifugation (green). C) Comparison of donor-acceptor ratios (I(565 nm)/I(515 nm)) after cryptand and 18-crown-6 addition. A lower concentration of cryptand is needed to unfold the G-quadruplex. D) FRET efficiencies calculated with FAM fluorescence decay times. Again, a lower concentration of cryptand is needed to unfold the G-quadruplex. Therefore, cryptand is used to perform further experiments.*

Influence of cryptand on FAM fluorescence

DNA origami structures modified only with FAM are analyzed after one cycle of KCl/cryptand addition. The fluorescence emission spectra and decays (Fig. S4) show that the FAM fluorescence is quenched after cryptand addition. The FAM emission intensity drops (Fig. S4 A, red) and the FAM fluorescence decay time decreases from 4.4 ns to 4.0 ns after cryptand addition (Fig. S4 B).

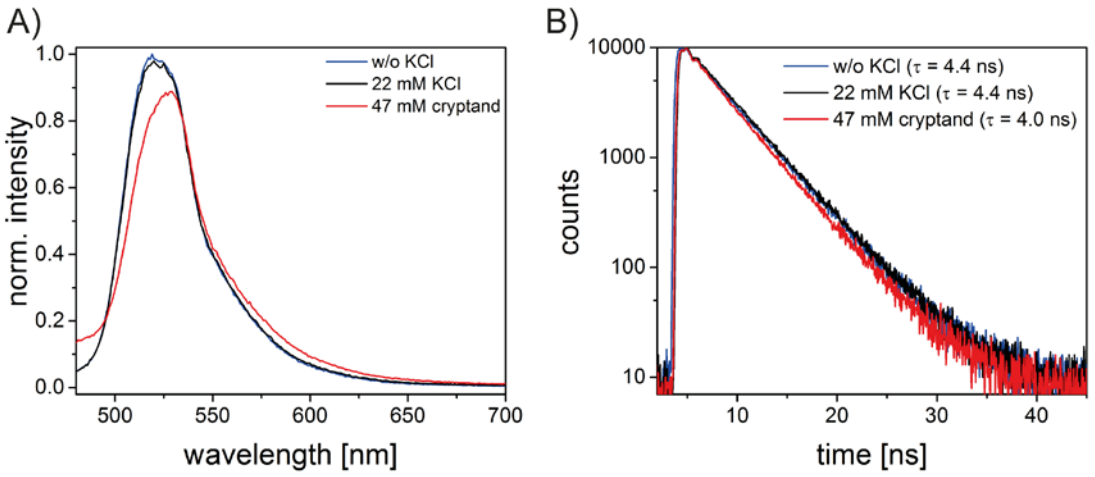

Fig. S 4 *Influence of cryptand on FAM fluorescence properties. A) Normalized emission spectra (λ_{ex} = 450 nm) of one sample before (blue), after KCl addition (black) and cryptand addition (red). The emission intensity decreases after cryptand addition. B) FAM fluorescence decays of one sample before (blue), after KCl (black) and after cryptand addition (red).*

Influence of cryptand on stability of DNA origami structures

For one sample the centrifugation step was carried out with a 100 kDa molecular weight cut-off filter instead of a 10 kDa molecular weight cut-off filter. The average fluorescence decay times of FAM and amplitudes of each decay time component are shown in Fig. S5. By using a 100 kDa molecular weight cut-off filter free DNA staple strands are removed from the solution (this is not the case when a 10 kDa molecular weight cut-off filter is used, 10 kDa < M(staple DNA) < 100 kDa). This can be confirmed with the time-resolved measurements. In Fig. S5 A the average FAM fluorescence decay time using all three decay time components is plotted.

$$\bar{\tau} = \frac{A_1 \cdot \tau_1 + A_2 \cdot \tau_2 + A_3 \cdot \tau_3}{A_1 + A_2 + A_3} \qquad (1)$$

The average fluorescence decay time decreases after KCl addition and it increases after cryptand addition. Furthermore, the amplitude of each decay time component is plotted in Fig. S5 B. It shows that the amplitude of the third decay time does not increase throughout repeating folding and unfolding cycles. In case of centrifugation steps using 10 kDa molecular weight cut-off filters the amplitude of the third decay time component increases continuously throughout the folding/unfolding experiments (see Fig. S6).

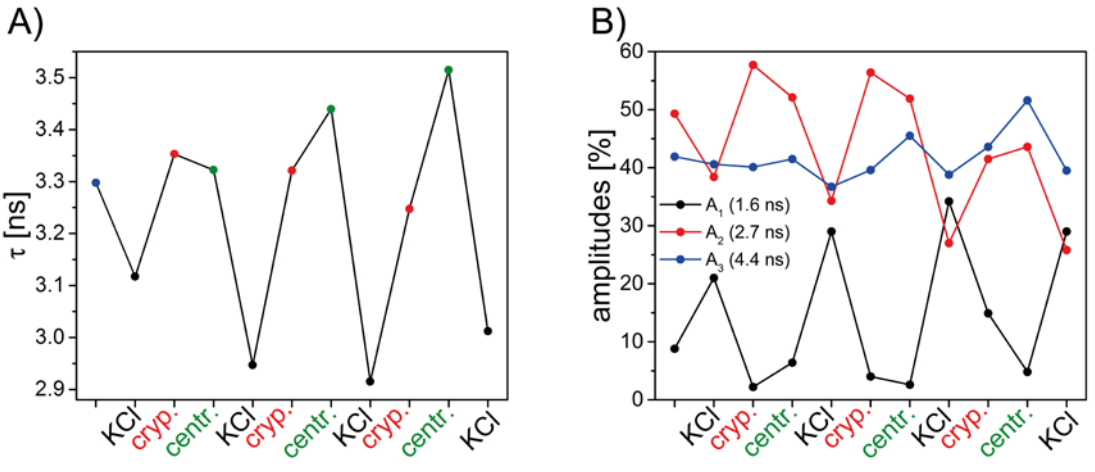

Fig. S 5 *Time-resolved measurements for centrifugation steps using 100 kDa molecular weight cut-off filter. A) Average fluorescence decay time calculated using all three decay time components. B) Amplitudes of each decay time component ($A_1 \rightarrow \tau_1$ (black); $A_2 \rightarrow \tau_2$ (red); $A_3 \rightarrow \tau_3$ (blue)).*

FAM fluorescence decay time

An overview of all determined fluorescence decay times and amplitudes for the two-color and three-color FRET systems are shown in Table S1. Additionally, the amplitudes for each fluorescence decay time component (two-color and three-color FRET systems) are plotted in Fig. S6. The diagrams show that the amplitude for the third decay time component (unquenched FAM) increases continuously throughout repeated folding-unfolding-cycles. This indicates that the DNA origami structures might dissociate and more free FAM labeled DNA strands are present.

Table S 1 *Overview of measured FAM fluorescence decay times. The fluorescence decay curves were fitted tri-exponentially with fixed τ values. The amplitudes for each decay time (A_1: τ_1 = 1.6 ns; A_2: τ_2 = 2.7 ns; A_3: τ_3 = 4.4 ns) and the average decay times calculated with the first two decay time components $\left(\bar{\tau} = \frac{A_1\tau_1 + A_2\tau_2}{A_1 + A_2}\right)$ for the two-color FRET system and three-color FRET cascade are depicted (with standard deviation of three separate measurements). The fluorescence decay times were measured at a KCl concentration of 22 mM and cryptand concentration of 47 mM.*

	Two-color FRET system				Three-color FRET cascade			
	A_1 [%]	**A_2 [%]**	**A_3 [%]**	**$\bar{\tau}$ [ns]**	**A_1 [%]**	**A_2 [%]**	**A_3 [%]**	**$\bar{\tau}$ [ns]**
	8.2 ± 0.9	49.6 ± 0.9	42.1 ± 1.8	2.54 ± 0.01	6.0 ± 0.9	74.3 ± 0.3	19.7 ± 1.2	2.62 ± 0.01
KCl	43.5 ± 3.1	19.4 ± 1.1	37.1 ± 2.4	1.94 ± 0.03	53.2 ± 4.4	25.6 ± 4.2	21.2 ±0.3	1.96 ± 0.06
crypt.	1.2 ± 0.6	52.3 ± 1.3	46.5 ± 1.6	2.68 ± 0.01	3.2 ± 3.2	59.8 ± 2.6	37.0 ±1.5	2.64 ± 0.05
centri.	6.0 ± 0.8	39.6 ± 3.9	54.4 ± 4.5	2.56 ± 0.01	4.8 ± 0.7	52.6 ± 0.5	42.7 ± 0.2	2.61 ± 0.01
KCl	28.5 ± 2.8	12.8 ± 2.0	58.6 ± 4.5	1.94 ± 0.03	28.1 ± 1.6	15.1 ± 4.5	56.8 ± 6.1	1.98 ± 0.07
crypt.	1.3 ± 0.6	39.8 ± 4.2	58.9 ± 4.1	2.67 ± 0.02	3.3 ± 2.3	41.5 ± 4.5	55.1 ± 4.1	2.62 ± 0.06
centri.	4.2 ± 0.9	33.2 ± 5.9	62.6 ± 6.7	2.58 ± 0.01	3.4 ± 1.0	35.3 ± 4.2	61.2 ± 5.1	2.60 ± 0.02
KCl	13.9 ± 7.2	8.2 ± 2.5	77.9 ± 5.6	2.04 ± 0.20	16.6 ± 2.8	9.3 ± 4.6	74.1 ± 3.1	1.99 ± 0.17
crypt.	2.2 ± 0.6	33.1 ± 2.1	64.7 ± 2.7	2.63 ± 0.01	3.5 ± 2.4	35.5 ± 3.8	61.0 ± 6.2	2.61 ± 0.05
centri.	4.3 ± 0.8	25.3 ± 8.4	70.4 ± 8.6	2.53 ± 0.04	1.3 ± 1.2	24.7 ± 5.9	74.1 ± 6.2	2.65 ± 0.04
KCl	13.2 ± 9.5	4.5 ± 3.1	82.3 ± 8.0	1.93 ± 0.22	13.2 ± 5.5	3.7 ± 3.5	83.1 ± 2.2	1.86 ± 0.25
crypt.	3.5 ± 2.3	30.0 ± 2.1	66.5 ± 4.3	2.59 ± 0.06	1.6 ± 0.6	26.6 ± 0.1	71.8 ± 0.5	2.64 ± 0.02
centri.	2.1 ± 1.8	19.8 ± 6.6	78.1 ± 5.8	2.58 ± 0.10	0.5 ± 0.1	12.7 ± 1.3	86.8 ± 1.4	2.66 ± 0.01
KCl	10.4 ± 9.5	5.3 ± 2.8	84.3 ± 11.2	2.02 ± 0.22	12.6 ± 3.1	2.8 ± 1.8	84.6 ± 4.8	1.79 ± 0.06

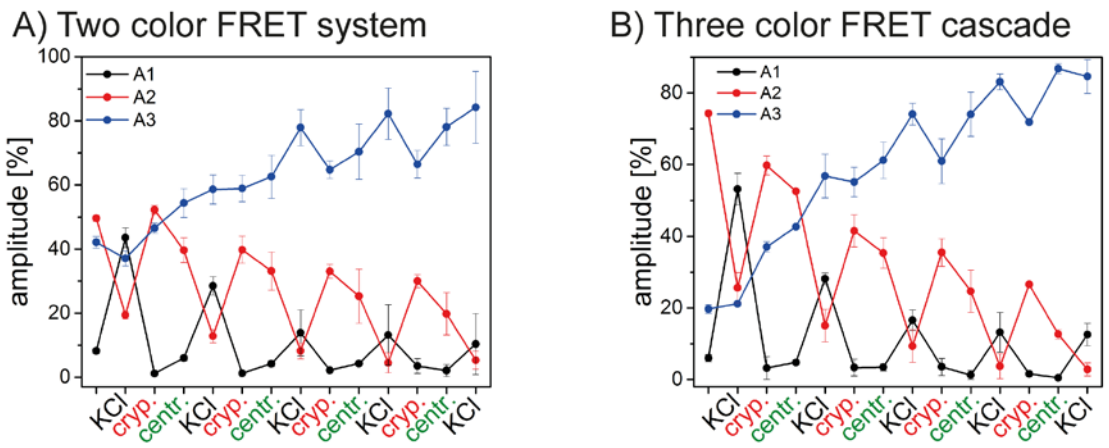

Fig. S 6 *Amplitudes of each fluorescence decay time component (A_1→ τ_1 (black); A_2→ τ_2 (red); A_3→ τ_3 (blue)) for the two-color FRET system (A) and three-color FRET cascade (B). The amplitude of A_3 increases throughout repeated folding and unfolding due to increasing amounts of free FAM labeled DNA strands.*

Decay associated spectra

Decay associated spectra are determined for the two-color FRET system to resolve the different contributions of the fluorescence emission spectra. The data are shown in Fig. S7 and Fig. S8. Fluorescence decay times have been measured at different emission wavelengths with an excitation

wavelength of 490 nm. The fluorescence decays are fitted tri-exponentially with fixed τ values for specific fluorescence decay times of FAM and Cy3, respectively. Since theses fluorescence decay times vary depending on KCl/cryptand concentration the fluorescence decays were fitted with different fixed decay time components (w/o salt/after centrifugation: τ_1(Cy3) = 1.9 ns, τ_2(FAM) = 2.7 ns, τ_3(FAM) = 4.4 ns; KCl: τ_1(FAM) = 1.6 ns, τ_2(Cy3) = 2.5 ns, τ_3(FAM) = 4.4 ns; cryptand: τ_1(Cy3) = 2.3 ns, τ_2(FAM) = 2.7 ns, τ_3(FAM) = 4.4 ns). The amplitudes for each decay time component are plotted in Fig. S7. The amplitudes of each decay time component are then multiplied with the normalized steady state emission spectra to obtain the deconvolved emission spectra (see Fig. S8). The acceptor-donor fluorescence intensity ratios are calculated based on the deconvolved data (Fig S8 D). The absolute values differ slightly from the raw data but the overall behavior stays the same. Thus, all other ratios are calculated based on raw data.

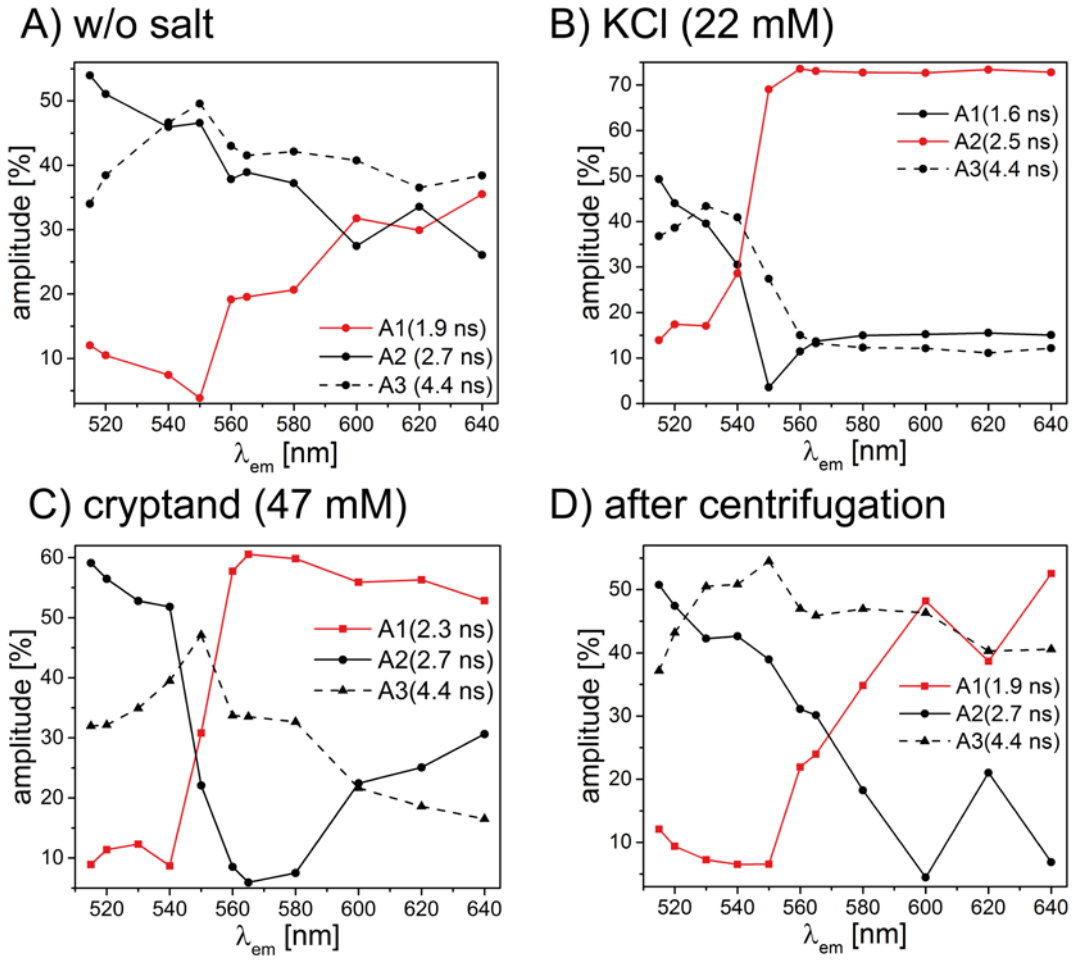

Fig. S 7 *Decay associated spectra of two-color FRET system of initial sample (A), after KCl addition (B), after cryptand addition (C) and after centrifugation (D). Amplitudes plotted for different decay time components (black: FAM: initial sample/cryptand/after centrifugation (unfolded telomere): τ_1 = 2.7 ns; KCl (folded G-quadruplex): τ_1 = 1.6 ns; unquenched FAM: τ_3 = 4.4 ns; red: Cy3: initial sample/after centrifugation: τ_1 = 1.9 ns; after KCl: τ_2 = 2.5 ns; after cryptand: τ_1 = 2.3 ns).*

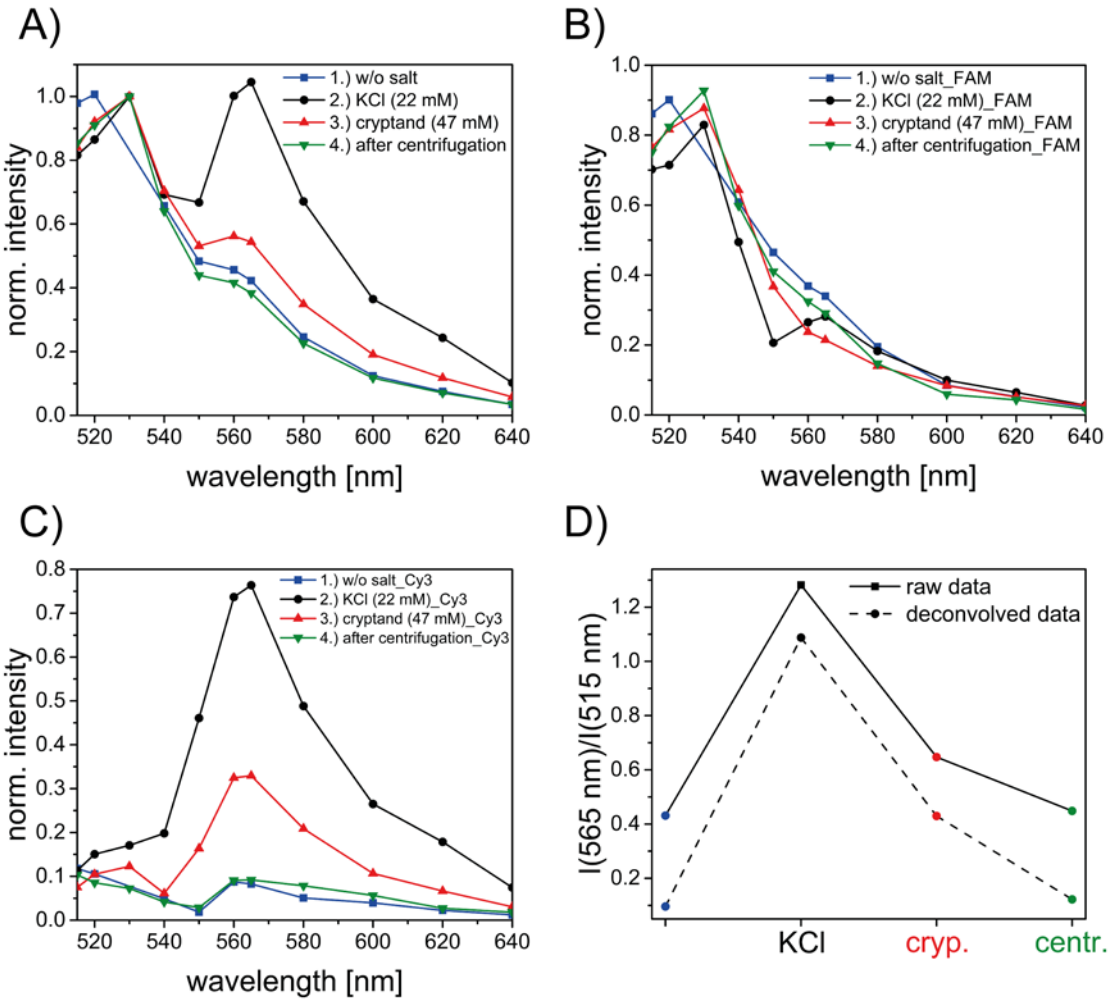

Fig. S 8 *Deconvolved emission spectra of two-color FRET system for one folding/unfolding cycle. Color code: blue: initial sample, black: after KCl addition, red: after cryptand addition, green: after centrifugation. A) Normalized steady state emission spectra without deconvolution. B) Deconvolved emission spectra for FAM. In the black spectrum a shoulder belonging to Cy3 is still visible. Peak at 530 nm belongs to the water Raman peak. C) Deconvolved Cy3 emission spectra. Emission belonging to Cy3 only is visible. D) Acceptor-donor ratios calculated with raw data (solid line) and deconvolved data (dashed line). Only the total values differ but not the overall behavior.*

FRET calculations

FRET is a non-radiative energy transfer from an excited donor to an acceptor molecule through dipole-dipole interactions. For FRET to take place two main conditions need to be fulfilled. Firstly, the donor's emission spectrum has to overlap with the acceptor's absorption spectrum (resonance condition, see Fig. S9). Secondly, the FRET pair needs to be in close proximity for FRET to take place. The FRET efficiency *E* is highly distance dependent and behaves according to the following equation.

$$E = \frac{R_0^6}{R_0^6 + R^6} \tag{2}$$

Here, *R* is the donor-acceptor distance and R_0 the Förster radius. The Förster radius is a FRET pair specific parameter at which the FRET efficiency is equal to 50 %. It depends on the spectral properties of donor and acceptor molecule and can be calculated using the following equations 3 and 4.

$$R_0^6 = \frac{9(ln10)\kappa^2 Q_D J}{128\pi^5 n^4 N_{AV}} \tag{3}$$

Where κ^2 is the dipole orientation factor, Q_D is the fluorescence quantum yield of the donor molecule when the acceptor is absent, N_{AV} is Avogadro's number, *n* is the medium's refractive index and *J* is the

spectral overlap integral representing the overlap of donor's emission and acceptor's absorption spectra. The spectral overlap integral is calculated using the following equation 4.

$$J(\lambda) = \int F_D(\lambda) \cdot \varepsilon(\lambda) \cdot \lambda^4 \, d\lambda \quad (4)$$

Here, $F_D(\lambda)$ is the normalized fluorescence emission spectrum of the donor at particular wavelength, $\epsilon(\lambda)$ is the acceptor's extinction coefficient spectrum in $l \cdot mol^{-1} \cdot cm^{-1}$ and λ is the wavelength in nm. The dipole orientation factor κ^2 takes on values between 0 and 4. For freely rotating molecules with a rotation rate much faster than the donor's de-excitation rate, κ^2 is equal to 2/3. [3–6]

The software PhotochemCAD 2.1 is used to calculate the spectral overlap integrals *J* and the Förster radius R_0 for each FRET pair (FAM-Cy3, Cy3-Cy5, FAM-Cy5, FAM-IRDye700, Cy3-IRDye700, Cy5-IRDye700). The desired spectra for the different FRET pairs (donor's emission spectrum and acceptor's absorption spectrum in terms of extinction coefficient, Fig. S9 A-F) are imported and the dipole orientation factor ($\kappa^2 = 2/3$), the refraction index (n = 1.33) and the specific quantum yield of the donor molecule ($Q(FAM)$ = 0.90; $Q(Cy3)$ = 0.15; Q(Cy5) = 0.30)[7] are used as inputs in the software. The calculated Förster radii are listed in Table S2.

FRET between FAM and Cy5 at a distance of ~7 nm is highly inefficient as shown in Fig. S10 (blue). Thus, Cy3 has to be introduced as a transmitter dye so that the energy is transferred from FAM to Cy3 followed by an energy transfer from Cy3 to Cy5.

Table S 2 *Overview of donor's quantum yield (Q_D), spectral overlap integral ($J(\lambda)$) and Förster radii (R_0) for the different FRET pairs.*

FRET-pair	Q_D[7]	$J(\lambda)$ [$nm^4 \cdot l \cdot mol^{-1}$]	R_0 [nm]
FAM-Cy3	0.90	$5.6 \cdot 10^{15}$	6.7
Cy3-Cy5	0.15	$7.4 \cdot 10^{15}$	5.2
FAM-Cy5	0.90	$3.1 \cdot 10^{15}$	6.1
FAM-IRDye700	0.90	$0.9 \cdot 10^{15}$	5.0
Cy3-IRDye700	0.15	$3.3 \cdot 10^{15}$	4.6
Cy5-IRDye700	0.30	$21.2 \cdot 10^{15}$	7.2

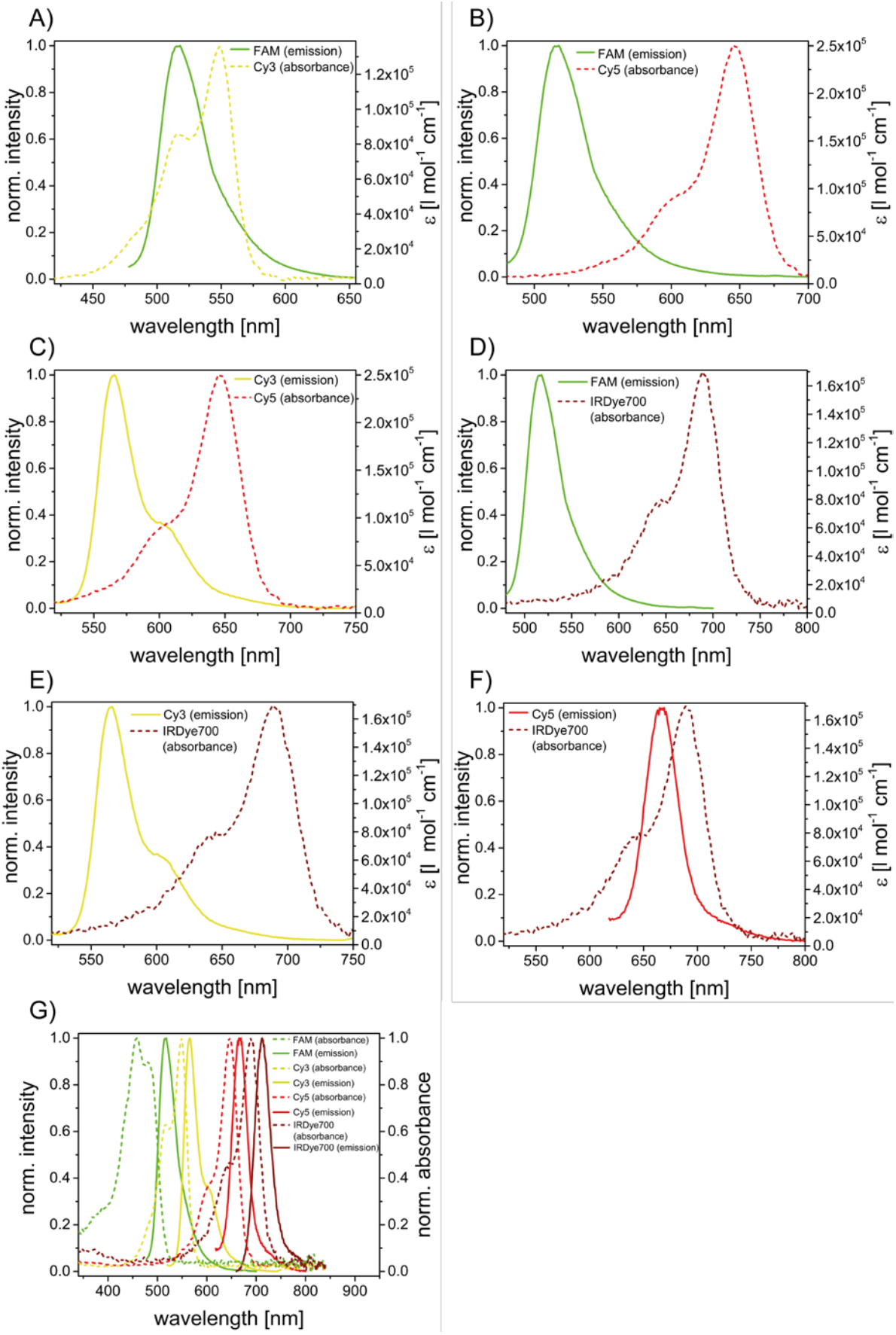

Fig. S 9 *Spectral overlap for each FRET pair (emission spectrum: solid line, absorption spectrum: dashed line). A) Large spectral overlap between FAM emission (donor, green) and Cy3 absorption spectra (acceptor, yellow). B) Small spectral overlap between FAM emission (donor, green) and Cy5 absorption spectra (acceptor, red). C) Large spectral overlap between Cy3*

emission (donor, yellow) and Cy5 absorption spectra (acceptor, red). D) Small spectral overlap between FAM emission (donor, green) and IRDye700 absorption spectra (acceptor, dark red). E) Small spectral overlap between Cy3 emission (donor, yellow) and IRDye700 absorption spectra (acceptor, dark red). F) Large spectral overlap between Cy5 emission (donor, red) and IRDye700 absorption spectra (acceptor, dark red). G) Spectral overlap of organic dyes used for the different FRET systems. Absorption (dashed line) and emission (solid line) spectra for donor molecule FAM (green), acceptor/transmitter molecule Cy3 (yellow), acceptor/transmitter molecule Cy5 (red) and acceptor molecule IRDye700 (dark red).

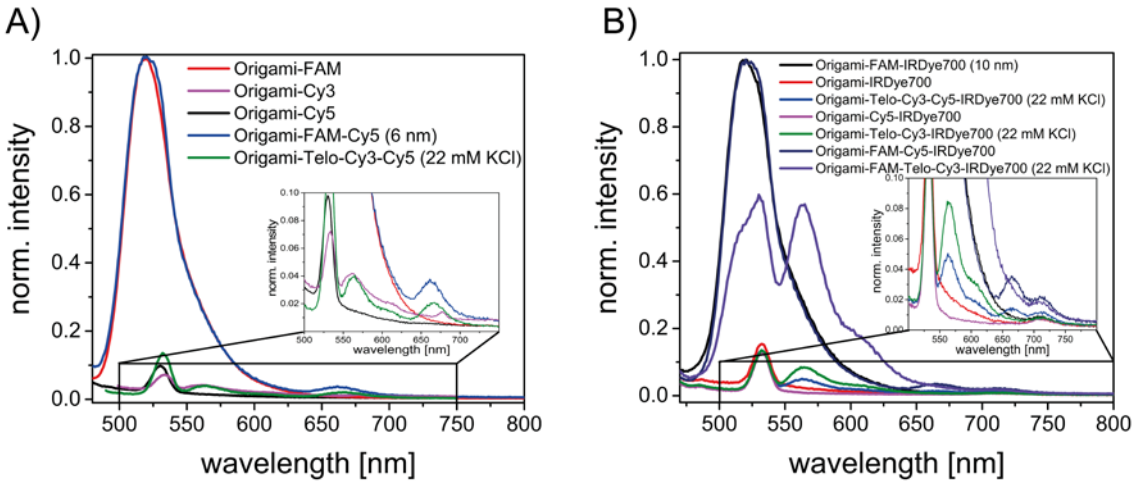

Fig. S 10 *Normalized emission spectra (λ_{ex} = 450 nm) for DNA origami structures modified with different organic dyes. A) Control experiments for two- and three-color FRET cascade for DNA origami structures modified with FAM (red), Cy3 (pink), Cy5 (black), FAM-Cy5 (blue) and RevHumTel-Cy3-Cy5 (green). Direct excitation of organic dyes other than FAM is neglectable. Weak emission of Cy5 at 665 nm in FAM-Cy5-sytsem (blue) is visible due to low energy transfer efficiency from FAM to Cy5. B) Control experiments for four-color FRET system. FAM-IRDye700 (black), IRDye700 (red), RevHumTel-Cy3-Cy5-IRDye700 (blue), Cy5-IRDye700 (pink), RevHumTel-Cy3-IRDye700 (green), FAM-Cy5-IRDye700 (dark blue), FAM-RevHumTel-Cy3-IRDye700 (violet). Direct excitation at 450 nm of organic dyes other than FAM is neglectable.*

Cy3 fluorescence decay time (three-color FRET cascade)

The Cy3 fluorescence decay time is analyzed in the three-color FRET cascade. The analysis of Cy3 fluorescence decay time is not trivial because it is influenced by many factors (G-quadruplex, FRET (enhancement by FAM, quenching by Cy5)). The fluorescence decay time of only Cy3 attached to the telomeric DNA on DNA origami structures increases significantly after KCl addition and decreases again after cryptand addition and centrifugation. The Cy3 fluorescence is known to be influenced by G-quadruplex structures due to association with the G-quadruplex.[8] The fluorescence decays of Cy3 are fitted bi-exponentially (τ_1 = 1.17 ns; τ_2 = 2.72 ns) and an average decay time based on the amplitudes is calculated. The decay curves and fluorescence decay times of origami structures only modified with Cy3 are plotted in Fig. S11 A-B. The fluorescence decay curves of Cy3 in the three-color FRET cascade are fitted tri-exponentially (τ_1 = 0.57 ns (FRET-component); τ_2 = 1.17 ns (Cy3); τ_3 = 2.72 ns (Cy3)) and the average fluorescence decay time is calculated based on the amplitudes. The fluorescence decay times are plotted in Fig. S11. The FRET efficiencies are calculated using equation 5.

$$E = 1 - \frac{\tau_{DA}}{\tau_D}, \qquad (5)$$

where τ_{DA} is the average fluorescence decay time when FRET occurs and τ_D is the Cy3 fluorescence decay time without FAM and Cy5 being present. Since τ_D depends strongly on KCl and cryptand the FRET efficiencies are calculated with the Cy3 fluorescence decay times measured in presence of KCl/cryptand (τ_D(KCl) = 2.6 ns; τ_D(cryptand) = 2.3 ns; τ_D(before/after centrifugation) = 1.9 ns) assuming that the Cy3 fluorescence decay time does not change throughout repeated folding/unfolding cycles. The calculated FRET efficiencies are plotted in Fig. S11 D. It has to be noted that since the Cy3 fluorescence decay time is highly influenced by KCl/cryptand addition and Cy3 and

Cy5 fluorescence decay times are quite similar (τ(Cy3) ≈ 2.2 ns, τ(Cy5) = 2.0 ns) the determined FRET efficiencies are somewhat error prone.

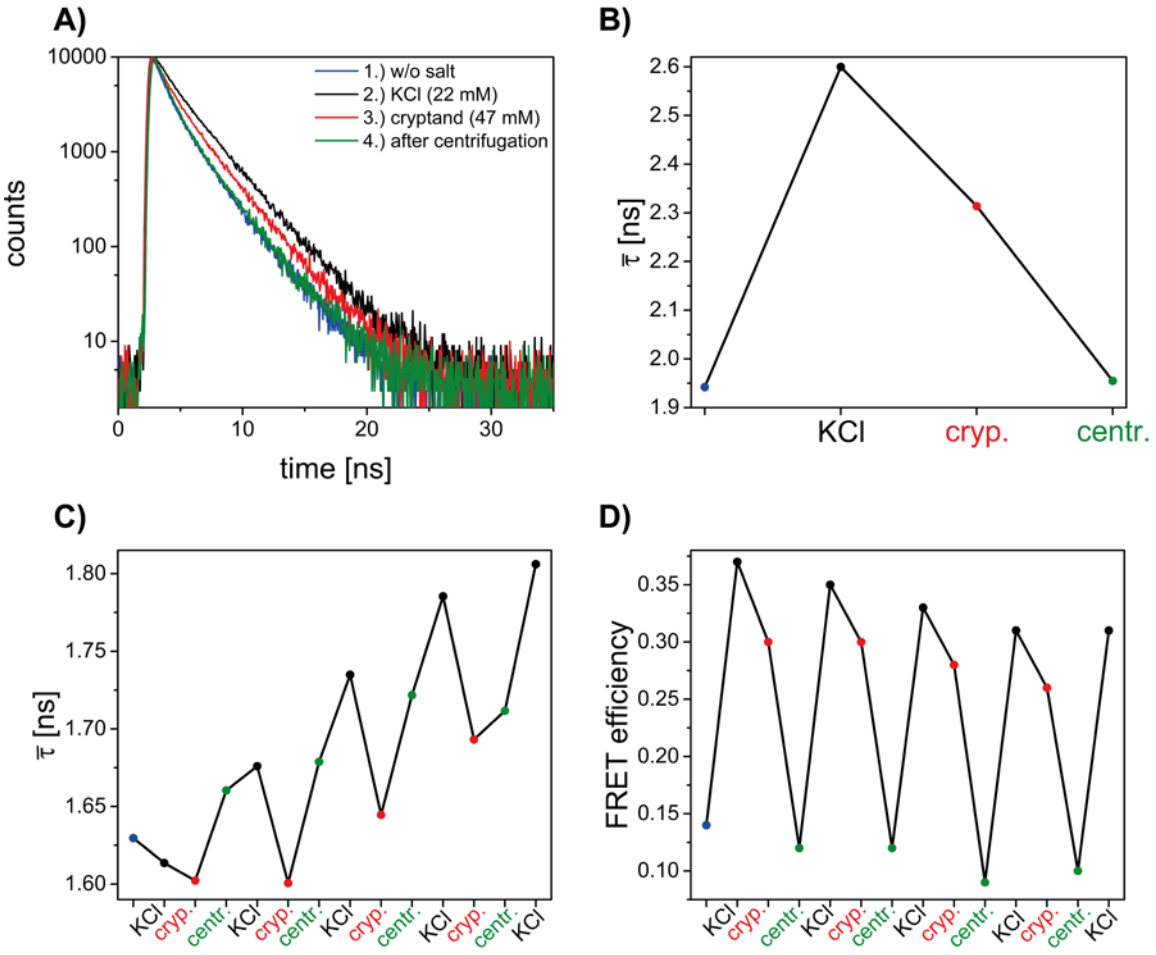

Fig. S 11 *Determination of Cy3 fluorescence decay times (λ_{ex} = 545 nm; λ_{em} = 565 nm). A) Fluorescence decays of DNA origami structures modified with Cy3 attached to RevHumTel. B) Determined fluorescence decay times of Cy3 attached to RevHumTel and immobilized on DNA origami structures. The Cy3 fluorescence decay time is highly influenced by KCl/cryptand addition. C) Average Cy3 fluorescence decay time of Cy3 in the three-color FRET cascade. D) FRET efficiencies calculated based on Cy3 fluorescence decay times.*

Four-color FRET photonic wire

To generally show the switching behavior of the four-color photonic wire two switching cycles are performed and shown in Fig. S12. The donor-acceptor ratios of each FRET pair (I(Cy3)/I(FAM); I(Cy5)/I(Cy3); I(Cy5)/I(FAM); I(IRDye700)/I(Cy5); I(IRDye700)/I(Cy3) and I(IRDye700)/I(FAM)) are shown in Fig. S12 B. Similar to the two- and three-color FRET systems they increase after KCl addition because of G-quadruplex formation and decrease after cryptand addition. The folding of the G-quadruplex can be repeated after centrifugation. It has to be noted that the IRDye700-Cy5-ratio behaves different than the others. This is because the distance between IRDye700 and Cy5 does not change during the G-quadruplex folding and unfolding process. Therefore, the overall FRET efficiency between these two dyes stays the same and only the Cy5 emission increases more strongly. FAM and Cy3 fluorescence decay times behave similarly compared to the three-color FRET system. The FAM fluorescence decay times and the FRET efficiencies based on FAM fluorescence decay times are exemplary shown in Fig. S12 C-D. Control experiments are shown in Fig. S13 to show that the FRET cascade is only efficient if all four organic dyes are present.

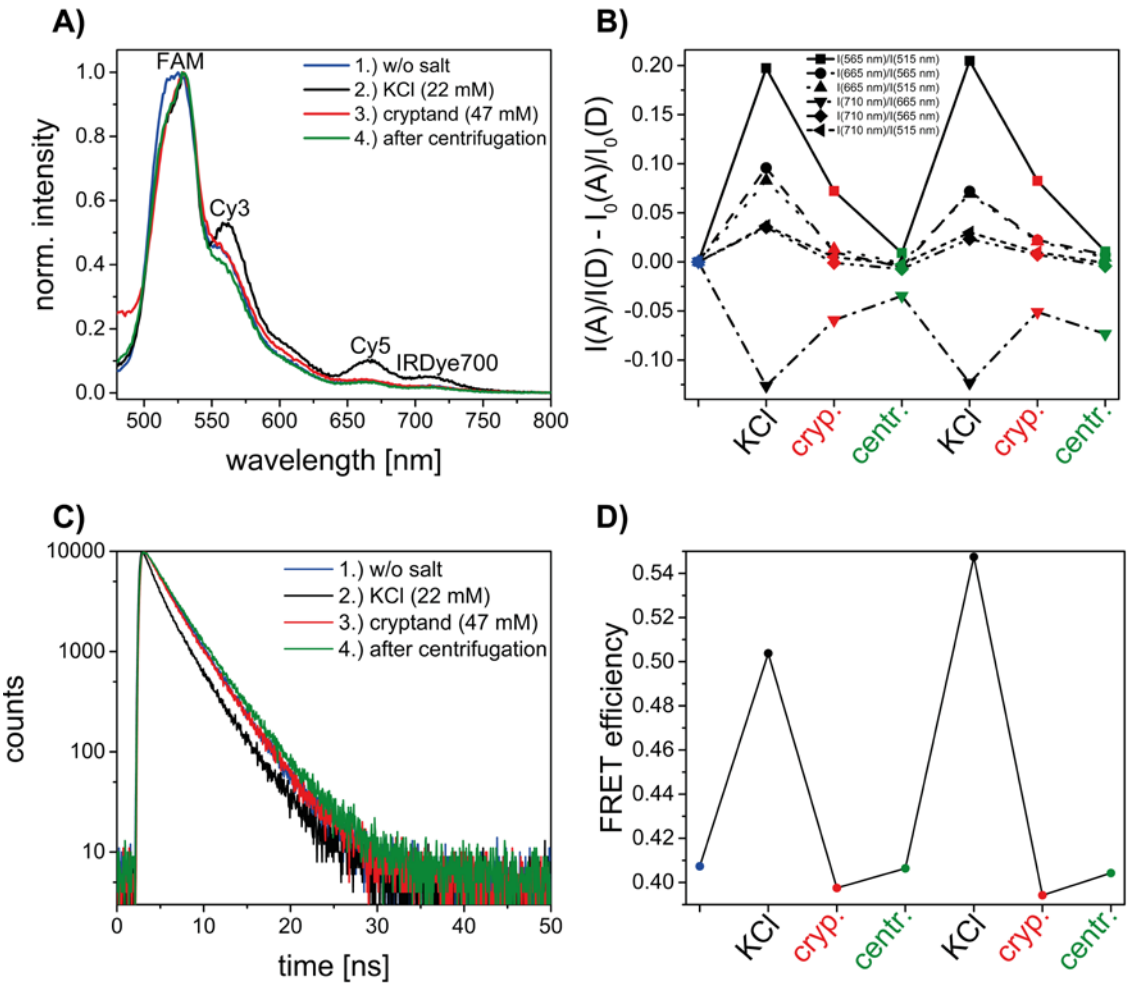

Fig. S 12 *Results for the four-color FRET photonic wire on DNA origami structures. A) emission spectra excited at 450 nm for one switching cycle (blue: initial sample, black: KCl, red: cryptand, green: after centrifugation). B) Calculated acceptor-donor ratios for each dye-pair. The ratios increase after KCl addition due to G-quadruplex formation and they decrease after cryptand addition due to G-quadruplex unfolding. The switching can be repeated. C) FAM fluorescence decay curves (λ_{ex} = 490 nm, λ_{em} = 520 nm) (blue: initial sample, black: KCl, red: cryptand, green: after centrifugation). D) FRET efficiencies based on FAM fluorescence decay times. The FRET efficiencies increase and decrease after KCl and cryptand addition, respectively*

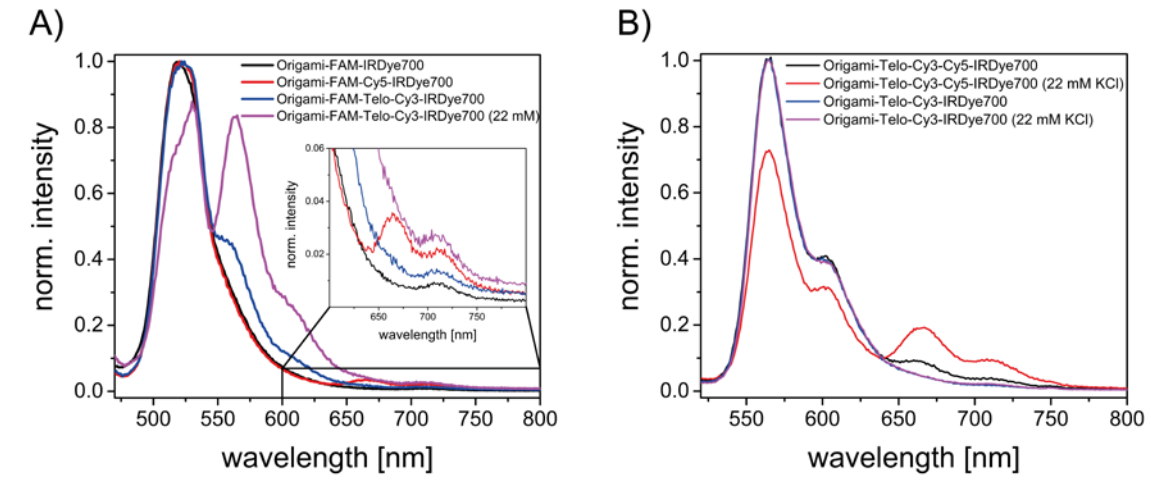

Fig. S 13 *Control experiments for the four-color FRET photonic wire. A) Steady state emission spectra with an excitation wavelength of 450 nm. Direct FRET from FAM to IRDye700 is very weak (black). FRET cascade is not working well if the first*

transmitter dye Cy3 is missing (red). If Cy5 is missing, the FRET cascade is also not working very efficient from FAM to Cy3 to IRDye700 (blue (w/o KCl), violet (KCl)). B) Switchable three-color FRET cascade (black) with Cy3 (donor), Cy5 (transmitter) and IRDye700 (acceptor). The FRET cascade is turned on after KCl addition (blue). FRET cascade is inefficient when Cy5 is missing (blue (w/o salt), violet (KCl)).

References

1 Kankia B., *Sci. Rep.*, 2015, **5**, 12996.
2 Yan Y.-Y., Lin J., Ou T.-M., Tan J.-H., Li D., Gu L.-Q. and Huang Z.-S., *Biochem. Biophys. Res. Commun.*, 2010, **402**, 614-618.
3 Förster T., *Naturwissenschaften*, 1946, **33**, 166-175.
4 Förster T., *Ann. Phys.*, 1948, **437**, 55-75.
5 Lakowicz J. R. *Principles of fluorescence spectroscopy.* 3rd ed. New York: Springer; 2006
6 Valeur B. and Berberan-Santos M. N. *Molecular Fluorescence: Principles and applications.* 2nd ed. Weinheim: Wiley-VCH; 2013
7 http://www.glenresearch.com//Technical/Extinctions.html
8 Søndergaard S., Aznauryan M., Haustrup E. K., Schiøtt B., Birkedal V. and Corry B., *Chemphyschem : a European journal of chemical physics and physical chemistry*, 2015, **16**, 2562-2570.